DOI: 10.1007/s41230-017-7077-z

Creep resistance of as-cast Mg-5Al-5Ca-2Sn alloy

Guang Zhang, *Ke-qiang Qiu, Qing-chun Xiang and Ying-lei Ren

School of Materials Science and Engineering, Shenyang University of Technology, Shenyang 110870, China

Abstract: In the present study, creep properties of as-cast Mg-5Al-5Ca-2Sn (AXT552) alloy were investigated by means of a GWT304 creep testing machine at temperatures of 175 °C and 200 °C in the stress range of 35–90 MPa. Results show that creep rates increase with applied stress at an identical temperature. Creep strain at 100 hours is 0.0518% and 0.083% at creep conditions of 175°C/75MPa and 200°C/60MPa, respectively, which is comparable to MRI230D and much lower than most of AX series alloys. By the observation and analysis for samples before and after creep tests using a Shimadzu XRD-7000 type X-ray diffractometer (XRD) and a Hitachi S-3400N type scanning electron microscope (SEM), it was found that Al_2Ca (C15) phase precipitated out of C36 phase or matrix. The cavity formation and connection at the interface of soft matrix and hard intermetallics caused the propagation of cracking along the eutectic phase during creep process and dislocation accommodated grain/phase boundary sliding is expected to be the dominant creep mechanism.

Key words: as-cast AXT552 alloy; creep properties; creep rate; creep strain; microstructure

CLC numbers: TG146. 22 **Document code:** A **Article ID:** 1672-6421(2017)04-265-07

Increasing attention has been paid due to increased demand of heat resistant magnesium alloys by heat-resistant parts, such as powertrain and transmission components [1] for lightweight vehicles. Mg-Al system is one focus for development of this kind of materials. In alloying elements, calcium makes a most attractive option since it provides acceptable levels of castability and increased corrosion and creep resistance at low cost in comparison with RE [2-4]. The addition of Ca to the Mg-Al system resulted in high pressure die casting MRI230D and MRI153 alloys, both of which present significantly better creep resistance than AE42 alloy [5,6]. Mg-Sn-based alloys have great potential for creep resistance because of the formation of thermally stable Mg_2Sn phase in the as-cast condition, and many Ca-containing Mg-Sn alloys exhibit good creep resistance [4, 7-11]. Therefore, the consideration for the development of Mg-Al-Sn-Ca alloy becomes necessary. In our previous studies, Mg-5Al-5Ca-2Sn (AXT552) presents good thermal stability [12] due to the formation of connected hard skeleton [13] composed of Al_2Ca and $(Mg,Al)_2Ca$ compounds. It was found that the skeleton is able to effectively shield load from the softer α-Mg matrix [14] and increase the creep resistance of the alloys [15,16]. Therefore, the tensile creep property of as-cast AXT552 alloy at temperatures of 175 °C and 200 °C was checked and compared with other heat-resistant Mg alloys in this study.

1 Experimental procedure

Mg-5Al-5Ca-2Sn (wt.%), or AXT552, alloy was prepared using commercial Mg, Al, Sn (with purity of 99.9%) metals and Mg-20Ca master alloy. The alloy was melted in a mild steel crucible under the protection of a mixed gas atmosphere of 1% SF_6 and 99% Ar. After the master alloy added was melted, the melt was held at 750 °C for 10 min, and then poured into a cylindrical mold made of cast iron with a diameter of 180 mm and height of 250 mm. The chemical composition of the ingots was determined by inductively coupled plasma analyzer (ICP) and the results were well consistent with the designed composition as shown in Table 1. The as-cast microstructure and phase constituent were analyzed and the details were given in the previous report [12,13].

Creep specimens with gauge dimensions of 3 mm × 6 mm × 27 mm were machined from these castings. Constant-load tensile creep tests were performed using

***Ke-qiang Qiu**

Male, born in 1962, Ph.D, Professor. His research interests mainly focus on the microstructure and properties of heat-resistant cast magnesium alloys and bulk metallic glasses.

E-mail: kqqiu@163.com

Received: 2017-03-29; Accepted: 2017-06-15

Table 1: Chemical compositions of AXT552 alloy (wt.%)

Composition	Mg	Al	Sn	Ca	impurity
Nominal composition	Bal.	5.0	2.0	5.0	-
Composition analyzed	Bal.	4.97	1.95	4.85	<0.6

a GWT304 creep testing machine at temperatures of 175 °C and 200 °C, respectively, in a stress range of 35–90 MPa. The temperature of the furnace was maintained constant to within ±2 °C during creep loading. Creep strain was measured by extensometers which were attached directly to the gauge section of specimens. Most tests were run under constant load to the final failure of specimens. The phase constituents before and after creep tests were analyzed by Shimadzu XRD-7000 type X-ray diffractometer (XRD). The surfaces of the fracture and the side near fracture points were observed using Hitachi S-3400N type scanning electron microscopy (SEM). Foils with 3 mm diameter for transmission electron microscope (TEM, JEOL JSM-7001F) observations were cut from the center of the creep specimens and then dimpled by a precision ion polishing system (PIPS Gatan) equipped with cooling system of liquid nitrogen.

2 Results and discussion

2.1 Creep properties of as-cast AXT552 alloy

The typical creep curves (strain *vs*. time) of the as-cast AXT552 alloy tested at temperatures of 175 °C [Fig. 1(a)] and 200 °C [Fig.1(b)] in the stress ranges of 75–90 and 35–75MPa, respectively, are shown in Fig. 1. For comparison, the creep curve with the lowest creep life at 200 °C is shown in the inset of Fig. 1(b). The creep life of 1,400 hours for the sample tested at stress of 35 MPa and temperature of 200 °C is not shown here due to one order longer than others. It is evident from the figures that all the curves exhibited a distinct primary (transient) creep regime followed by a steady state (secondary) creep and then the tertiary stage of the creep fracture process. At 175 °C, the creep rupture time had the following sequence for the three loading: 75MPa > 80MPa > 90MPa, with the creep rupture time of 127,

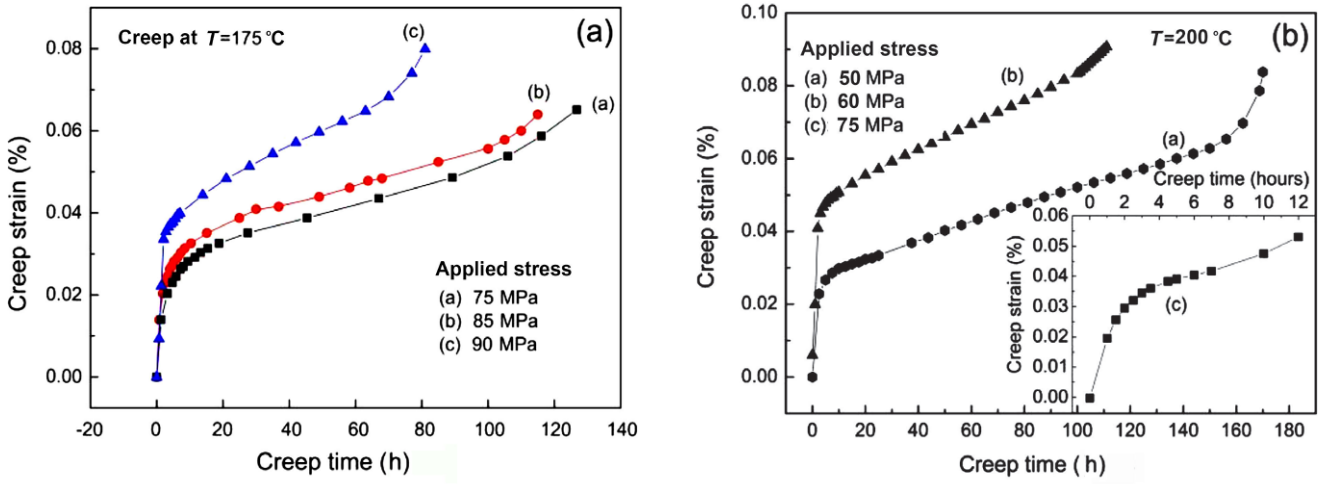

Fig. 1: Creep strain-creep time curves for AXT552 alloy tested at temperature of 175 °C (a) and 200 °C (b), respectively

115 and 81 h, respectively. While at 200 °C, the creep rupture time followed the same sequence of 1,400, 170, 111 and 12 hours for the loading of 35, 50, 60 and 75 MPa , respectively. For the same load of 75 MPa, the rupture time for the sample crept at 200 °C was quite lower than that obtained at 175 °C, indicating the temperature sensitivity of the alloy. However, the strain increased rapidly when the creep strain increased from 50 to 60 MPa at 200 °C, this also indicates the stress sensitivity of the alloy.

The creep rate (strain rate) was calculated from the steady state region of the strain vs. time curves for all the specimens, i.e., from the second stage in each case. The calculation of strain rate values based on the linear fit in the steady state region of the creep plots in Fig. 1 are shown in Fig. 2.

It was noticed from the values shown in Fig. 2 that the creep rate increased with applied stress at an identical temperature. At

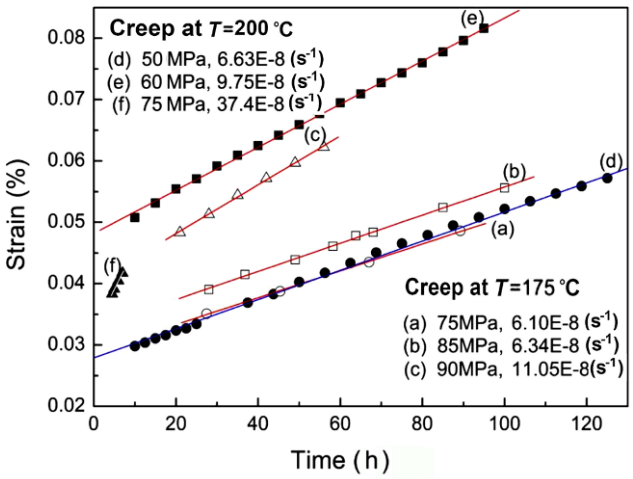

Fig. 2: Calculation of strain rate by linear fit to strain *vs*. time plots shown in Fig. 1

the creep temperature of 175 °C, the creep rate increased by only 0.24 when the applied stress is increased from 75 to 85 MPa, and the increase became significant at stress of 90 MPa. It is obvious that the increase in the creep rate is more significant for the samples crept at 200 °C. It was increased by a factor of 5.64 when the applied stress was increased from 50 to 75 MPa. A similar trend was also found when the temperature was raised from 175 to 200 °C at the same applied stress of 75 MPa. The creep rates for the lowest and the highest ones varied by a factor of 6.13. In general, the specimen tested at the lower temperature or stress exhibits a relatively longer primary creep stage than those tested at higher temperature or higher stress. For comparison, the creep rate was obtained by differentiating creep strain shown in Fig. 1 with respect to creep time and was plotted against creep time (t) normalized by the rupture time (t_r) (Fig. 3). It was found that the creep rates decreased rapidly during initial creep stage: the lower the creep life, the faster the decrease of the creep rate. No constant creep rate was observed even if the steady stage was assumed, which indicated that strain and strain (creep) rate followed different rules during creep processes. Creep rates reached the minimum at about 1/2 of the rupture time for the specimens tested at 175 °C independent of stress [Fig. 3(a)], while the minimum creep rate was seen at about 2/3, 1/2 and 1/2 of the rupture time for the specimens tested 200 °C under stress of 50, 60 and 75 MPa, respectively [Fig. 3(b)]. The creep rate increased after the minimum creep rate was reached and the increase became rapid during tertiary stage of creep. The shape of the creep rate curves reflects microstructural changes such as dynamic precipitation, which is related to the degree of solute supersaturation in the matrix [1]. Therefore, it was inferred no significant microstructure change for the samples tested at creep temperature of 750 °C due to almost no shape change for the time dependence of creep rate curves, while the microstructure for the samples crept at 200 °C under stresses of 50 and 60 MPa, respectively, should be different, which will be discussed in the following section.

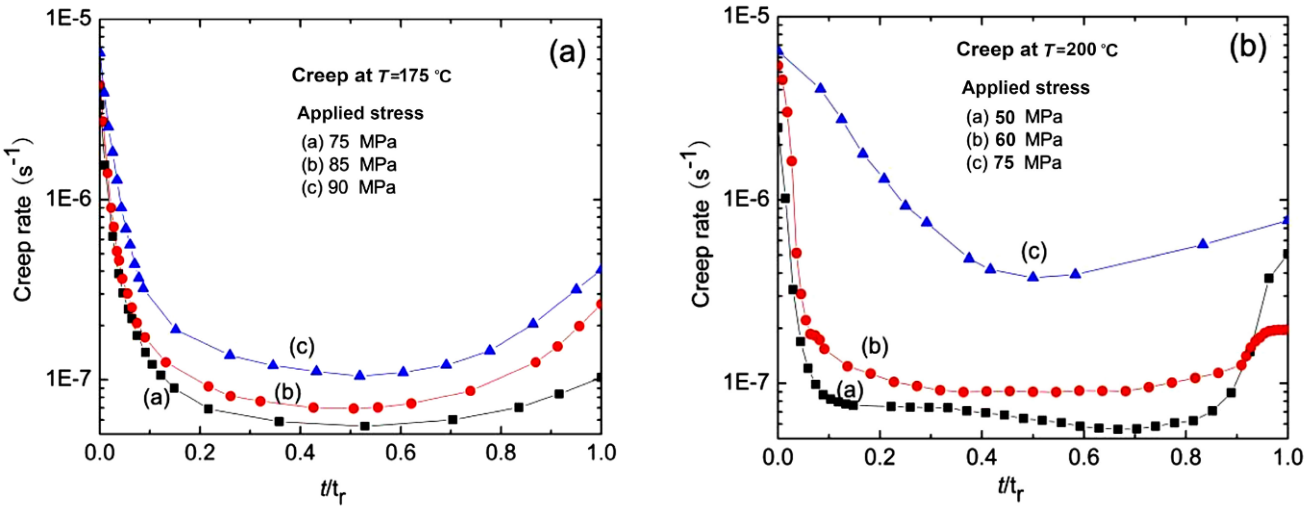

Fig. 3: Creep rate vs. time normalized by rupture time for AXT552 at 175 °C (a) and 200 °C (b), respectively

The creep properties of heat resistant magnesium alloy are usually described by the secondary creep rate and creep strain of 100 hours [1, 5, 17-19], therefore, the comparison between different heat resistant magnesium alloys is necessary. Table 2 summarizes the most important RE-free magnesium alloys, including the famous MRI230D [5], AJX series [17,18] alloys. In order to narrow the difference in experimental conditions, only those with similar creep experimental conditions are given in Table 2, including the present study on AXT552 alloys crept at conditions of 175°C/75MPa and 200°C/60MPa for comparison. At 175 °C, the applied stress used in the creep tests for most of the alloys was 70 MPa. The stress applied to MRI153 alloy was 90 MPa, but it crept at a lower temperature of 150 °C, therefore, the creep condition of 175°C/75MPa used in our experiments was more severe than other alloys. However, at 200 °C, the creep condition was less severe than other alloys. Considering the corresponding creep rates for AXT552, MRI230D, MRI153 and ATX421 alloys, the creep properties for the four alloys were comparable in terms of secondary creep rate. We also noticed that the creep rate for AXT552 was about two order lower than AJX511, AJX611, AX52 and AX53 alloys. However, the creep strain of 100 hours for AXT552 was smaller than that of most of the alloys listed in the table except the creep strain of AJX611 at 175 °C. Therefore, we can say that AXT552 presents better creep property in terms of creep rate and creep strain.

2.2 Microstructure observation before and after creep tests

Figure 4 shows the XRD patterns obtained from AXT552 alloy in the as-cast (Fig. 4a), as-crept at conditions of 175°C/85MPa [Fig. 4(b)], 200°C/50MPa [Fig. 4(c)] and 200°C/60MPa [Fig. 4(d)], respectively. From the XRD patterns, the constituent phases of as-cast alloy are composed of α-Mg, $(Mg,Al)_2Ca$, Al_2Ca and CaMgSn, which is in accordance with our previous

Table 2: Secondary creep rate and creep strain of 100 hours for some heat-resistant magnesium alloys

Alloys	Creep rate (s^{-1})/Stress (MPa)		100 h creep strain (%)		Sources
	175 °C	200 °C	175 °C	200 °C	
MRI230D	3.92×10^{-8}/70	1.28×10^{-7}/70	0.24*	-	[5]
AJX511	~9×10^{-10}/70	~2.5×10^{-9}/70	~0.1	~0.18	[17]
AJX611	~5×10^{-10}/70	~5×10^{-9}/70	~0.03	~0.2	[17]
AX52	6.95×10^{-10}/70	3.43×10^{-9}/56	0.06	0.26	[18]
AX53	8.64×10^{-10}/70	5.64×10^{-9}/56	0.09	0.28	[18]
AX53+0.15Sr	5.56×10^{-10}/70	1.11×10^{-9}/56	0.08	0.16	[18]
ATX421	2.4×10^{-8}/70**	-	2.1***	-	[19]
AT42	2.39×10^{-7}/70**	-	15.4***	-	[19]
MRI153	~4×10^{-8}/90**		3.8		[1]
AXT552	6.1×10^{-8}/75	6.63×10^{-8}/50	0.0518	0.0521	Present work
	6.34×10^{-8}/85	9.75×10^{-8}/60	0.0558	0.0830	Present work

*200 h creep strain; **creep at 150 °C; ***150 h creep strain

research[12]. Comparison between the patterns obtained before and after creep tests from the alloy revealed that there was no new phase formation in the alloy during creep exposure. However, the intensity of the peaks corresponding to the Al_2Ca phase is increased when the creep temperature is 200 °C, while there is almost no change for the sample tested at 175 °C. It should be noticed that the AXT552 alloy has a multi-phase structure and the volume fraction of some intermetallic phases is low, therefore, the XRD analysis for some phases, such as CaMgSn, is not obvious. An additional complication is the similarity of the crystal structures of the $(Mg,Al)_2Ca$ (C36) and Mg_2Ca (C14) phases, resulting in the peaks belonging to these Laves compounds overlapping in the XRD pattern. Therefore, the co-existence of C36 and C14 phases is possible. The stability of the intermetallic C36 phase during annealing at 300 °C was examined in die-cast Mg-5Al-3Ca based alloys. The C36 phase transformed to the C15 (Al_2Ca) phase by a shear-assisted mechanism [20]. Precipitates of the C15 Laves phase were also found within the α-Mg grains in die-cast Mg-5Al-3Ca-0.15Sr alloy as a result of aging in the temperature range from 175 °C to 350 °C [21]. Therefore, the precipitates assisted by both the temperature and applied stress under creep condition become possible and the peak intensity corresponding to C15 phase will increase in the XRD patterns. Figure 5 presents the TEM image of the precipitates for the sample crept at 200 °C and applied stress of 60 MPa. According to the electron diffraction pattern (inset of Fig. 5) and the morphology described by the literatures [22], the needle-like phase existed in or near C36 phase is C15

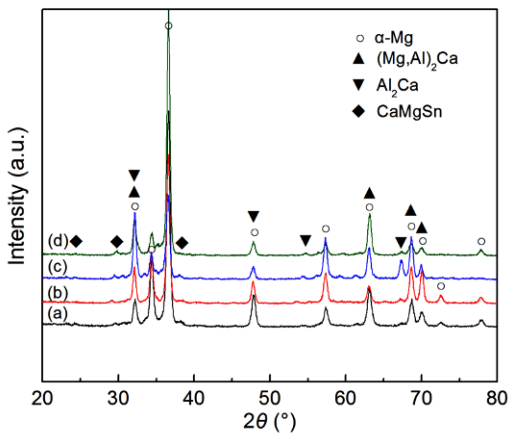

Fig. 4: XRD patterns for as-cast (a), as-crept at conditions of 175°C/85MPa (b), 200°C/50MPa (c) and 200°C/60MPa (d), respectively

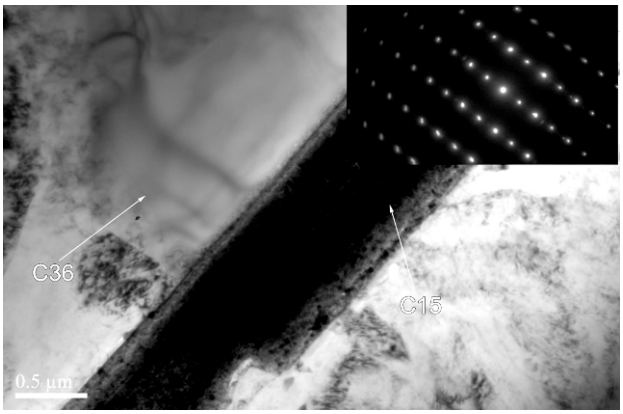

Fig. 5: TEM bright field image and electron diffraction pattern (inset of the figure) of needle-shaped Al_2Ca (C15) phase, [110] zone axis

phase. Therefore, the intensification of the Al_2Ca phase peak during creep test is attributed to its dynamic precipitation.

The microstructure changes before and after creep tests are shown in Fig. 6. It is seen from Fig. 6(a) that the primary α-Mg grains of as-cast AXT552 alloy are surrounded by the interconnected network of the grain boundary phase. This phase, which forms during the eutectic solidification process, has a lamella-type or irregular morphology, which can be found in the previous studies [12,13]. The crystal structure of the eutectic compound $(Mg,Al)_2Ca$ has been identified as irregular C36 and/or lamellar C14 structure in many as-cast AX series alloys [1,22,24,25]. The microstructure near the rupture surface for

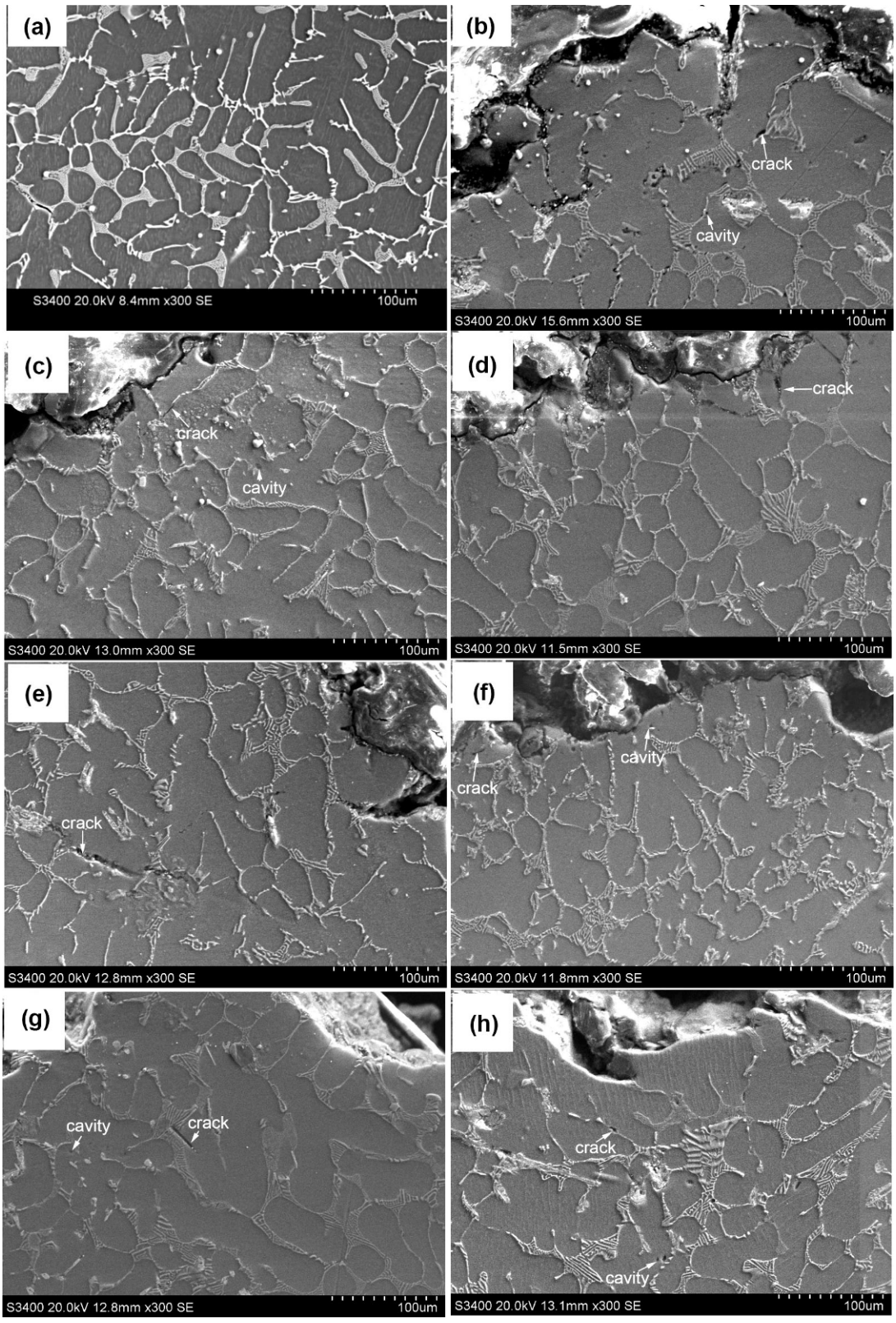

Fig. 6: Microstructures of as-cast (a) and as-crept samples at creep conditions of 175°C/75MPa (b), 175°C/85MPa (c), 175°C/90MPa (d), 200°C/35MPa (e), 200°C/50MPa (f), 200°C/60MPa (g), 200°C/75MPa (h)

the samples crept at 170 °C under stress of 75, 85 and 90 MPa is shown in Fig. 6(b), (c) and (d), respectively. It is obvious that the size of α-Mg cells is increased by ~10%, but there is no much change for the microstructure. The failure mode for samples tested at 175 °C and different stresses is the cracking between α-Mg and eutectic phase as indicated by the arrows shown in Fig. 6(b), (c) and (d), respectively. At the same time, the cracking sites shown in Fig. 6(b) are more numerous and further away from the fracture compared to other samples as shown in Fig. 6(c) and (d) due to exposures for the longest time at the same creep temperature of 175 °C. A similar situation was observed in Fig. 6(e) for the sample tested at 200°C/35MPa creep condition with creep life over 1,400 hours. This phenomenon indicates that the lower the stress, the more homogeneous deformation will occur for the creep sample at an identical temperature. The microstructure changes for the samples tested at 200 °C are somewhat dependent of the applied stress, i.e., the microstructure for the sample tested at the lowest stress of 35 MPa [Fig.6(e)] is comparable to the as-cast alloy, while at the higher stresses, such as 50, 60 and 70 MPa [Figs. 6(f), (g) and (h)], the microstructure changes have taken place to some extent. The irregular eutectic phase in Fig. 6(f) became discontinuous or the lamella-type eutectic phase in Fig. 6(g) became indistinct, while shear flow in both the eutectic phase and the matrix was observed in Fig. 6(h). The discontinuous and indistinct eutectic phase is possibly related to the phase change of eutectic, such as C15 precipitates from C39 as shown in Fig. 5. The shear flow near fracture surface was blocked up by eutectic phase which is shown in Fig. 7(a) as the magnification of Fig. 6(h), indicating that the fracture for the sample is non-uniform at high stress and high temperature. The microstructure of eutectic phase in the shear area (left) and un-shear area (right) is obviously different.

The rugged fracture surfaces shown in Fig. 6(e) and (f) indicate that the cracks extend along the interface between eutectic phase and the matrix. Figure 7(b) shows the crack initiation in $(Mg, Al)_2Ca$ compounds as indicated by arrows, which was also observed by Xu et al [25] in a Mg-Al-Ca alloy system. It is obvious that the many tiny cavities are induced to form at or near the interface, between intermetallics and matrix, where dislocations as indicated by an arrow can be seen. Cavity formation was also observed as a precursor of creep fracture as shown in Fig. 6(h). Most of the cavities formed owing to stress concentration at phase boundaries, triple points and/or interface between a soft phase and hard intermetallic phase. The connection and extension for those cavities cause the fractue of the creep samples. From the above analysis, we can see that the dominant creep mechanism is phase boundary cracking and sliding, which results in grain movements accommodated with either diffusion or with dislocation motion. Therefore, dislocation-accommodated grain boundary sliding is expected to be the dominant creep mechanism.

The higher heat resistance for AXT552 alloy can be attributed to the formation of hard connected skeleton structure with high thermal stability as reported [12,13] previously. The skeleton is able to effectively shield load from the softer α-Mg matrix and increase the creep resistance of the alloys [14-16]. Therefore, very few dislocations could be observed as indicated by Fig. 7(b). Certainly dislocation can be observed at fracture sites where high stress concentration exists. Away from the fracture point, however, cavity formation caused by dislocation piled up will in turn result in the submergence of the dislocation.

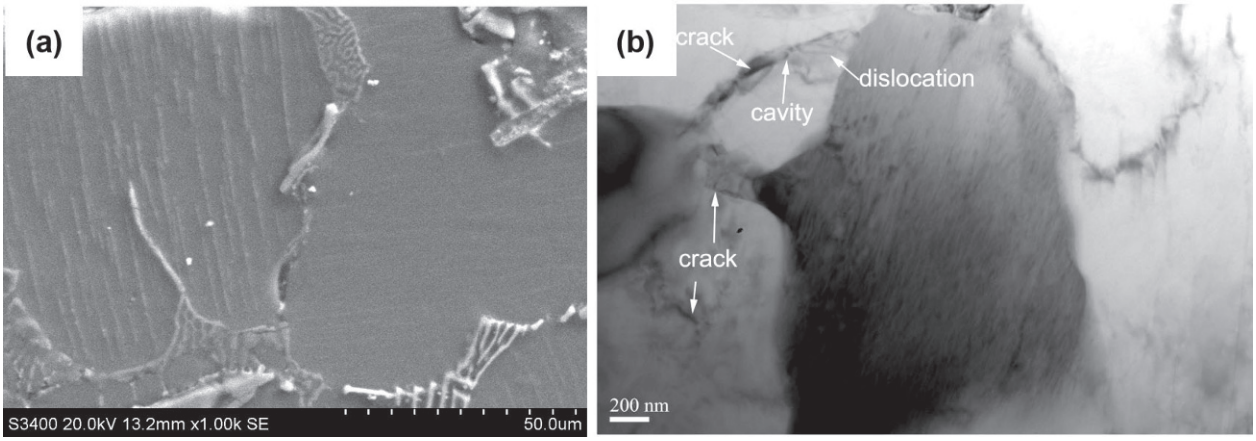

Fig. 7: SEM image showing microstructure near fracture site for sample crept at 200°C/75MPa (a) and TEM image showing cavity formation at interface between intermetallics and matrix (b)

3 Conclusions

(1) The secondary creep rates for AXT552 alloy tested at 175 °C are 6.1×10^{-8}, 6.34×10^{-8} and 1.1×10^{-7} s^{-1} under applied sresses of 75, 85 and 90 MPa, respectively, and they are increased to 6.63×10^{-8}, 9.75×10^{-8} and 3.7×10^{-7} s^{-1} under applied sresses of 50, 60 and 75 MPa, respectively, at creep temperature of 200 °C.

(2) The creep strain of 100 hours for AXT552 alloy at creep conditions of 175°C/75MPa, 175°C/85MPa, 200°C/50MPa and 200°C/60 MPa is 0.0518, 0.0558, 0.0521 and 0.083%, respectively, which is much lower than most RE-free heat resistant magnesium alloys in related to similar creep conditions.

(3) The cavity formation and connection cause the cracking along the interface between eutectic phase and the matrix. Dislocation-accommodated grain boundary sliding is the dominant creep mechanism.

References

[1] Zhu S M, Mordike B L and Nie J F. Creep properties of a Mg-Al-Ca alloy produced by different casting technologies. Mater. Sci. Eng. A, 2008, 483–484: 583–586.
[2] Zakiyuddin A and Lee K. Effect of a small addition of zinc and manganese to Mg-Ca based alloys on degradation behavior in physiological media. J. Alloy. Compd, 2015, 629: 274–283.
[3] Nie J F and Muddle B C. Precipitation hardening of Mg-Ca(-Zn) alloys. Scr. Mater., 1997, 37 (10): 1475–1481.
[4] Khalilpour H, Miresmaeili S M and Baghani A. The microstructure and impression creep behavior of cast Mg-4Sn-4Ca alloy. Mater. Sci. Eng. A, 2016, 652: 365–369.
[5] Mondal A K, Kesavan A R and Reddy B R K, et al. Correlation of microstructure and creep behaviour of MRI230D Mg alloy developed by two different casting technologies. Mater. Sci. Eng. A, 2015, 631: 45–51.
[6] Nami B, Rashno S and Miresmaeili S M. Effect of tin on the microstructure and impression creep behavior of MRI153 magnesium alloy. J. Alloy. Compd., 2015, 639: 308–314.
[7] Hasani G H and Mahmudi R. Tensile properties of hot rolled Mg-3Sn-1Ca alloy sheets at elevated temperatures. Mater. Des, 2011, 32: 3736–3741.
[8] Yang M, Ma Y and Pan F. Effects of little Ce addition on as-cast microstructure and creep properties of Mg-3Sn-2Ca magnesium alloy, Trans. Nonferrous Met. Soc., 2009, 19: 1087–1092.
[9] Liu H, Chena Y, and Tang Y, et al. The microstructure, tensile properties, and creep behavior of as-cast Mg-(1-10)%Sn alloys. J. Alloy. Compd, 2007, 440: 122–126.
[10] Hort N, Huang Y and Leil T A, et al. Microstructural investigations of the MgSnxCa system. Adv. Eng. Mater, 20 and, Miresmaeili S M. Impression creep behavior of a cast MRI153 magnesium alloy. Mater. Des., 2014, 60: 289–294.
[12] Qiu K Q, Zhang H H and Re Y, et al. Formation and thermal stability of connected hard skeleton structure in ATX525 cast alloys. China Foundry, 2015,12(6): 412–417.
[13] Re Y, Qiu K Q and Ren Y L, et al. Effect of heat treatment on morphology evolution of CaMgSn phase in ATX525 magnesium alloy. Trans. Mater. Heat Treatment, 2015, 36(4): 98–103.
[14] Amberger D, Eisenlohr and Göken M. On the importance of a connected hard-phase skeletonfor the creep resistance of Mg alloys. Acta Mater., 2012, 60: 2277–2289.
[15] Pekguleryuz M O and Renaud J. Creep Resistance in MgAlCa Alloys. 2000 Magnesium Technology, Kaplan H, Hryn J, Clow B, Eds. TMS, 2000, 279–84.
[16] Blum W, Eisenlohr P and Zeng X H, et al. Creep of Mg-alloys. Pekguleryuz M O, Mackenzie L W F, Eds. Magnesium Technology in the Global Age. Metallurgy and Petroleum, Canadian Institute of Mining; 2006: 633–646.
[17] Bai J, Sun Y S and Xue F, et al. Effect of Al contents on microstructures, tensile and creep properties of Mg-Al-Sr-Ca alloy. J. Alloy. Compd, 2007, 437: 247–253.
[18] Luo A A, Balogh M P and Powell B R. Creep and microstructure of magnesium-aluminum-calcium based alloys. Metall. Mater. Trans. A, 2002, 33: 567–577.
[19] Kim B H, Jo S M and Lee Y C, et al. Microstructure, tensile properties and creep behavior of Mg-4Al-2Sn containing Ca alloy produced by different casting technologies. Mater. Sci. Eng. A, 2012, 535: 40–47.
[20] Suzuk A, Saddock N D and Jones J W, et al. Solidification paths and eutectic intermetallic phases in Mg-Al-Ca ternary alloys. Acta Mater., 2005, 53: 2823–2834.
[21] Suzuki A, Saddock N D and Riester L, et al. Effect of Sr additions on the microstructure and strength of a Mg-Al-Ca ternary alloy. Metall. Mater. Trans. A, 2007, 38 (2): 420–427.
[22] Rzychon T. Characterization of Mg-rich clusters in the C36 phase of the Mg-5Al-3Ca-0.7Sr-0.2Mn alloy. J. Alloy. Compd., 2014, 598: 95–105.
[23] Suzuki A, Saddock N D and Jones J W, et al. Structure and transition of eutectic $(Mg,Al)_2Ca$ Laves phase in a die-cast Mg-Al-Ca base alloy. Scr. Mater., 2004, 51: 1005–1010.
[24] Ozturk K, Zhong Y and Luo A A, et al. Creep resistant Mg-Al-Ca alloys. Computational thermodynamics and experimental investigation. JOM, 2003, 55: 40–44.
[25] Xu S W, Matsumoto N and Yamamoto K, et al. High temperature tensile properties of as-cast Mg-Al-Ca alloys. Mater. Sci. Eng. A, 2009, 509: 105–110.